Applied Mathematics Letters 111 (2021) 106652

Contents lists available at ScienceDirect

Applied Mathematics Letters

www.elsevier.com/locate/aml

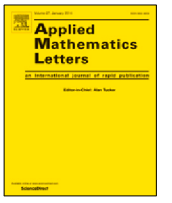

A stabilized finite element method for the Poisson–Nernst–Planck equations in three-dimensional ion channel simulations

Qin Wang [a,b], Hongliang Li [c,*], Linbo Zhang [a,b], Benzhuo Lu [a,b,**]

[a] *LSEC, NCMIS, Academy of Mathematics and Systems Science, Chinese Academy of Sciences, Beijing 100190, China*
[b] *School of Mathematical Sciences, University of Chinese Academy of Sciences, Beijing 100049, China*
[c] *Department of Mathematics, Sichuan Normal University, Chengdu 610066, China*

ARTICLE INFO

Article history:
Received 23 May 2020
Received in revised form 22 July 2020
Accepted 22 July 2020
Available online 28 July 2020

Keywords:
Poisson–Nernst–Planck
Stabilized finite element method
SUPG
interior penalty

ABSTRACT

The Poisson–Nernst–Planck (PNP) model characterizing the electro-diffusion process is widely used in ion channel simulations. The standard finite element method often fails to converge, due to complicated geometries, strong fixed charges and huge bias of electric potentials or ion concentrations. We propose a novel stabilized finite element method named SUPG–IP, which inherits the upwind characteristic of the streamline-upwind/Petrov–Galerkin (SUPG) method and the smoothing effect of the interior penalty method. Numerical experiments have demonstrated that the SUPG–IP method has much better performance in positivity preserving and robustness than the standard FE and SUPG methods. Especially, the benchmark simulation of the KcsA ion channel implies that the SUPG–IP method still converges successfully under an unprecedented range of membrane potentials and ion concentrations, while the SUPG method diverges.

1. Introduction

The Poisson–Nernst–Planck (PNP) model is widely used to characterize the electro-diffusion process of ions in electrolyte solution. Compared with discrete models, such as molecular dynamics model [1] and Brownian dynamics model [2], the PNP model has higher computational efficiency and is convenient to extract macroscopic properties of certain biological systems such as current–voltage characteristics and conductance rectification. Analogous models were developed in simulations of semiconductor devices [3] and nanopores.

The molecular surface geometry of an ion channel, which is usually highly irregular, sorely affects the transport behavior of ions in the channel. The finite difference [4] and finite volume methods [5] are two popular numerical methods, because they have advantage in implementation and preservation of numerical

* Corresponding authors.
** Correspondence to: No. 55 Zhongguancun East Road, Haidian District, Beijing 100190, China.
E-mail addresses: lihongliang@lsec.cc.ac.cn (H. Li), bzlu@lsec.cc.ac.cn (B. Lu).

https://doi.org/10.1016/j.aml.2020.106652
0893-9659/

flux, respectively. However, performance of the above two methods for simulations of three-dimensional ion channels always suffers from poor mesh quality. The finite difference method prefers regular structured meshes and the finite volume method prefers Delaunay meshes. The finite element (FE) method [6] is a natural choice for discretization of the PNP model in ion channel simulations, for its lower requirements for mesh quality. Actually, it is difficult to mesh a three-dimensional ion channel, especially to obtain high-quality mesh. Lu's group has developed a specific mesh generation tool chain [7] based on the software TMSmesh [8] for membrane-channel protein systems. Then ion channel simulations with FE discretization can be implemented efficiently. However, simulation with a large electrostatic potential is still a challenging problem, because the PNP model turns to be a convection-dominated problem. Moreover, for ion channel systems, complicated geometries of proteins, along with singularity of permanent charges, lead to rapid changes of the electrostatic potential and ionic concentrations around the protein surface, which greatly increases the difficulty of simulation.

As we know, there usually exist internal layers or exponential boundary layers in the exact solution of the convection-dominated model. A common approach to overcoming such difficulty is to employ the "upwind technique" in numerical schemes. One of the most successful and extensively used stabilized FE methods is the streamline-upwind/Petrov–Galerkin (SUPG) method [9], which introduces a streamline upwind perturbation to the standard Galerkin weighting function. When employing the SUPG method in actual ion channel simulations, we find that it also has the phenomenon of non-physical oscillations, i.e., the ionic concentrations may appear negative and lead to divergence of numerical solution. Motivated by the SUPG method and the interior penalty (IP) method [10,11], we propose a novel stabilized FE method for the PNP model, which is named SUPG–IP. The IP method adds a penalizing term corresponding to gradient jumps across element boundaries to enforce a smoother solution. The SUPG–IP method inherits the "upwind" characteristic of the SUPG method and the smoothing effect of the IP method. We test the performance of the standard FE, SUPG and SUPG–IP methods, and the details will be presented in a later section. A benchmark test on the KcsA ion channel implies that the SUPG–IP method has unexpected robustness, which succeeds in converging under an unprecedented range of membrane potentials and bulk concentrations while the SUPG method fails.

The rest of the paper is organized as follows: In Section 2, we introduce the PNP model and the basic setup of ion channel simulations. The novel SUPG–IP method is constructed and detailed algorithms of the PNP model are presented as well. Numerical performance of the standard FE, SUPG and SUPG–IP methods can be found in Section 3. Our work is summarized in Section 4.

2. Materials and methods

2.1. The Poisson–Nernst–Planck model for ion channels

Let $\Omega \subset \mathbb{R}^3$ denote an open domain. The subdomain $\Omega_m \subset \Omega$ represents the solute region, i.e., the protein and membrane region, with an outer boundary Γ_m, and the remaining space $\Omega_s = \Omega \setminus \bar{\Omega}_m$ represents the solvent region, including the channel, with an outer boundary Γ_s. The two subdomains are separated by a molecular interface Γ, i.e., $\Gamma = \partial\Omega_s \bigcap \partial\Omega_m$. A two-dimensional illustration of the model system in a simulation box is shown in Fig. 1.

The Nernst–Planck equations are as follows:

$$\frac{\partial c_i}{\partial t} = \nabla \cdot D_i(\nabla c_i + \beta\nabla(q_i\phi)c_i) + f_i, \text{ in } \Omega_s, \ i = 1, \ldots, K, \tag{1}$$

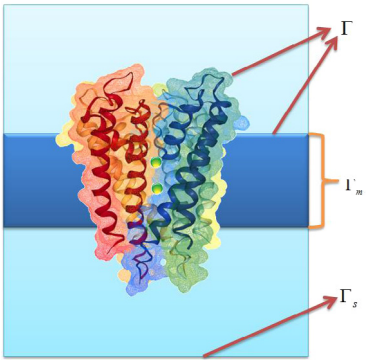

Fig. 1. A cut plane through the center of the simulation box along the z axis.

and the Poisson equation with internal interface Γ reads as:

$$-\nabla\cdot\epsilon\nabla\phi=\rho^f+\lambda\sum_{i=1}^{K}q_ic_i,\ \text{in }\Omega, \tag{2}$$

$$\phi_m=\phi_s,\ \epsilon_m\frac{\partial\phi_m}{\partial\boldsymbol{n}}=\epsilon_s\frac{\partial\phi_s}{\partial\boldsymbol{n}},\ \text{on }\Gamma, \tag{3}$$

where ϕ and K stand for the electrostatic potential and the number of multiple ion species, respectively. ϵ is the piecewise dielectric constant with $\epsilon=\epsilon_m\epsilon_0$ in Ω_m and $\epsilon=\epsilon_s\epsilon_0$ in Ω_s, where ϵ_0 is the dielectric constant of vacuum. In ion channel systems, typical values of ϵ_m and ϵ_s are 2 and 80, respectively. $\rho^f=\sum_k q_k\delta(x-x_k)$ is an ensemble of fixed charges q_k located at x_k. λ is the indicator function of Ω_s. $q_i=z_ie_c$ specifies the charge carried by each particle of the ith ion species with e_c for the elementary charge. c_i is the concentration of the ith ion species and D_i is the corresponding diffusivity. $\beta=1/(k_BT)$ is the inverse Boltzmann energy, where k_B is the Boltzmann constant and T is the absolute temperature. f_i are the source terms. $\boldsymbol{n}$ is the unit normal of the interface Γ pointing from Ω_m to Ω_s. In this paper, since our focus is on the space discretization, we will only study the steady state, i.e., $\partial c_i/\partial t=0$.

The system is augmented with the following boundary conditions:

$$\phi=\phi_D,\qquad \text{on }\Gamma_{D,\phi}, \tag{4}$$

$$c_i=c_{i,D},\qquad \text{on }\Gamma_{D,c_i},\ i=1,\dots,K, \tag{5}$$

$$\nabla\phi\cdot\boldsymbol{n}=0,\qquad \text{on }\Gamma_{N,\phi}, \tag{6}$$

$$\boldsymbol{J}_i\cdot\boldsymbol{n}=0,\qquad \text{on }\Gamma_{N,c_i},\ i=1,\dots,K, \tag{7}$$

where $\boldsymbol{J}_i=-D_i(\nabla c_i+\beta\nabla(q_i\phi)c_i)$. $\boldsymbol{n}$ is the outward unit normal of the boundary. $\Gamma_{D,\phi}$, $\Gamma_{N,\phi}$ and Γ_{D,c_i}, Γ_{N,c_i} refer to the Dirichlet boundary and the Neumann boundary for the electrostatic potential and ionic concentrations, respectively.

To deal with singular permanent charges, an effective strategy is to decompose the electrostatic potential into three components: a singular component G, a harmonic component H and a regular component ϕ^r with G and H restricted to Ω_m [6]. The final PNP equations consist of the regularized Poisson equation with an interface condition:

$$-\nabla\cdot\epsilon\nabla\phi^r=\lambda\sum_{i=1}^{K}q_ic_i,\ \text{in }\Omega, \tag{8}$$

$$\phi_m^r=\phi_s^r,\ \epsilon_s\frac{\partial\phi_s^r}{\partial\boldsymbol{n}}-\epsilon_m\frac{\partial\phi_m^r}{\partial\boldsymbol{n}}=\epsilon_m\left(\frac{\partial G}{\partial\boldsymbol{n}}+\frac{\partial H}{\partial\boldsymbol{n}}\right),\ \text{on }\Gamma, \tag{9}$$

and the steady-state NP equations:

$$-\nabla\cdot D_i(\nabla c_i+\beta\nabla(q_i\phi^r)c_i)=f_i,\ \text{in }\Omega_s,\ i=1,\dots,K. \tag{10}$$

For simplicity, we introduce a new variable $u=e_c\beta\phi^r$ to nondimensionalize the electrostatic potential. Then the steady-state PNP equations become:

$$-\nabla\cdot\epsilon\nabla u=e_c^2\beta\lambda\sum_{i=1}^{K}z_ic_i,\qquad \text{in }\Omega, \tag{11}$$

$$-\nabla\cdot D_i(\nabla c_i+z_ic_i\nabla u)=f_i,\quad \text{in }\Omega_s,\ i=1,\dots,K. \tag{12}$$

2.2. The SUPG–IP stabilized finite element method

In this subsection, we will discuss a novel stabilized finite element method for the coupled PNP equations in detail. We decouple the nonlinear system (11)–(12) by Gummel iteration. In each iteration, the Poisson equation and each NP equation are solved successively. The ionic concentrations are treated as given functions when solving the electrostatic potential, and vice versa. The process is repeated until the change of the solutions in two adjacent iterations becomes smaller than a given tolerance.

Define $H_u^1(\Omega)=\{v\in H^1(\Omega):v|_{\Gamma_{D,\phi}}=0\}$. The weak form of the Poisson equation (11) is to find $u\in H^1(\Omega)$ satisfying the Dirichlet boundary condition (4) such that

$$\int_\Omega\epsilon\nabla u\cdot\nabla\varphi d\Omega=e_c^2\beta\int_\Omega\lambda\sum_{i=1}^{K}z_ic_i\varphi d\Omega-e_c\beta\int_\Gamma\epsilon_m\left(\frac{\partial G}{\partial\boldsymbol{n}}+\frac{\partial H}{\partial\boldsymbol{n}}\right)\varphi d\Gamma,\quad\forall\varphi\in H_u^1(\Omega). \tag{13}$$

Here Γ is the molecular interface and $\boldsymbol{n}$ is the unit normal of Γ pointing from Ω_m to Ω_s. The weak form of the NP equation for the ith ($i=1,\dots,K$) ion species (12) is to find $c_i\in H^1(\Omega)$ satisfying the Dirichlet boundary condition (5) such that

$$A(c_i,v):=\int_\Omega D_i(\nabla c_i+z_ic_i\nabla u)\cdot\nabla v d\Omega=\int_\Omega f_iv d\Omega,\quad\forall v\in H_{c_i}^1(\Omega), \tag{14}$$

where $H_{c_i}^1(\Omega)=\{v\in H^1(\Omega):v|_{\Gamma_{D,c_i}}=0\}$. Stabilization is imposed on the NP equations. Define the Peclet number Pe as an indication for convection intensity:

$$Pe_T=\frac{\|\boldsymbol{b}_i\|_2h_T}{2D_i},$$

where $\boldsymbol{b}_i=-D_iz_i\nabla u$ is the velocity field. h_T is the diameter of the element T and Pe_T denotes the value of Pe in T. Let $\mathcal{F}_h^{\text{int}}$ be the set of the interior element boundaries. The stabilization term and the corresponding right-hand side term are defined as:

$$S(c_i,v):=\sum_T\int_T\big(-\nabla\cdot D_i(\nabla c_i+z_ic_i\nabla u)\big)v_{\text{stab}}dT+\sum_{F\in\mathcal{F}_h^{\text{int}}}\alpha\tau_{i,F}\int_F[\nabla c_i\cdot\boldsymbol{n}][\nabla v\cdot\boldsymbol{n}]dF,$$

$$L(v):=\sum_T\int_T f_iv_{\text{stab}}dT,$$

where $v_{\text{stab}}=\sigma_T\boldsymbol{b}_i\cdot\nabla v$. The stabilizing parameter σ_T is defined based on Pe:

$$\sigma_T=\frac{h_T}{2\|\boldsymbol{b}_i\|_2}\xi(Pe_T),\quad\xi(Pe_T)=\begin{cases}Pe_T/3, & 0\le Pe_T\le 3,\\ 1, & Pe_T>3.\end{cases}$$

α is a positive constant and $\boldsymbol{n}$ is the outward unit normal of F. The stabilizing parameter $\tau_{i,F}$ is motivated by [12] and defined as follows:

$$\tau_{i,F} := \frac{h_F^3 \|\boldsymbol{b}_i\|_{L^2(F)}^2}{\|\boldsymbol{b}_i\|_{L^2(F)} h_F + D_i},$$

where h_F is the diameter of F. Then the weak form of the NP equation after stabilization is to find $c_i \in H^1(\Omega)$ satisfying the Dirichlet boundary condition (5) such that

$$A(c_i, v) + S(c_i, v) = \int_\Omega f_i v d\Omega + L(v), \quad \forall v \in H^1_{c_i}(\Omega). \tag{15}$$

3. Results and discussion

3.1. Numerical accuracy tests

We carry out a suite of test problems to examine the accuracy and robustness of the SUPG–IP method and compare it with the standard FE and SUPG methods. All the numerical algorithms are implemented based on the three-dimensional parallel finite element toolbox Parallel Hierarchical Grid (PHG) [13]. The parameter α in the SUPG–IP method is set to 0.02, which is determined by numerical experiments to achieve optimal performance in balance of accuracy and robustness.

Example 1. In this example, we solve a problem with an analytical solution. The open domain Ω is specified as a $[0\,\mathring{A},\ 1\,\mathring{A}]^3$ cube. Two charged species K^+ and Cl^- are considered in the system. The analytical solution for the concentrations of the charged species is defined as follows:

$$c_1(x, y, z) = \tau_1 + \frac{\tau_1}{2}\cos(\pi x)\cos(\pi y)\cos(\pi z), \quad c_2(x, y, z) = \tau_1 - \frac{\tau_1}{2}\cos(\pi x)\cos(\pi y)\cos(\pi z), \tag{16}$$

where $\tau_1 = 0.05$ M. The analytical solution for the electrostatic potential consists of two parts ϕ_1 and ϕ_2:

$$\phi(x, y, z) = \phi_1(x, y, z) + \phi_2(x, y, z), \tag{17}$$

where

$$\phi_1(x, y, z) = \tau_2 \cos(\pi x)\cos(\pi y)\cos(\pi z), \quad \phi_2(x, y, z) = \tau_3 z.$$

τ_3 is set to 0.1 V. ϕ_2 is a linear function of z and does not contribute to the Poisson equation. τ_2 is calculated to make the Poisson equation satisfied. Substitution of the solution (16) for ionic concentrations in the NP equations produces the source terms f_i and boundary data. The boundary conditions for the electrostatic potential are set with Dirichlet boundary conditions on the top and bottom faces of the cube and Neumann boundary conditions on the lateral faces. For the NP equations, Dirichlet boundary conditions are prescribed on all the faces.

We solve the example problem on five grids with elements bisected three times successively. The results are displayed in Table 1. The second column presents times of bisection. Obviously, the relative errors decrease as times of refinement increase. The relative errors and convergence orders of the SUPG–IP method are comparable to those of the SUPG method. After three times of refinement, the L^2 norms of the relative errors of the SUPG–IP scheme are all less than 3.0×10^{-4}, verifying its accuracy and applicability to three-dimensional PNP modeling.

Example 2. In this example, we strengthen the convection term by raising the voltage applied. Ionic concentrations are increased simultaneously to make the problem more challenging. This time we consider

Table 1
The L^2 norms of the relative errors of the SUPG and SUPG–IP methods.

Method	Grid	$\|\|\phi_h - \phi\|\|$	Order	$\|\|c_{1h} - c_1\|\|$	Order	$\|\|c_{2h} - c_2\|\|$	Order
SUPG	0	5.842024e−08	–	6.980832e−04	–	6.793810e−04	–
	3	2.304957e−08	1.3417	2.968621e−04	1.2336	2.951311e−04	1.2029
	6	8.507302e−09	1.4380	1.133355e−04	1.3892	1.129783e−04	1.3853
	9	2.052790e−09	2.0511	2.905586e−05	1.9637	2.901428e−05	1.9612
	12	5.422815e−10	1.9205	7.576687e−06	1.9392	7.570478e−06	1.9383
SUPG–IP	0	5.845009e−08	–	6.988103e−04	–	6.799854e−04	–
	3	2.305302e−08	1.3422	2.969473e−04	1.2347	2.952093e−04	1.2038
	6	8.507593e−09	1.4381	1.133463e−04	1.3895	1.129893e−04	1.3856
	9	2.052790e−09	2.0512	2.905660e−05	1.9638	2.901503e−05	1.9613
	12	5.422814e−10	1.9205	7.576736e−06	1.9392	7.570528e−06	1.9383

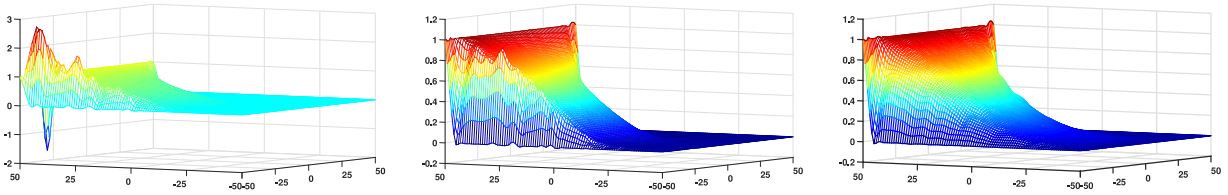

Fig. 2. Concentration distributions of K^+ on the yOz cut plane. Left: standard FE method. Center: SUPG method. Right: SUPG–IP method.

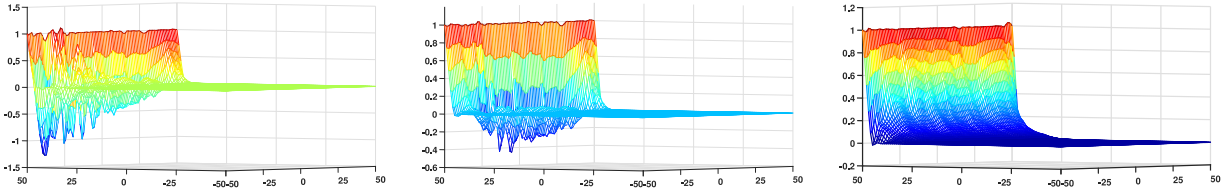

Fig. 3. Concentration distributions of Cl^- on the yOz cut plane. Left: standard FE method. Center: SUPG method. Right: SUPG–IP method.

a $[-50\,\mathring{A},\, 50\,\mathring{A}]^3$ cube with the charged species K^+ and Cl^- as well. The source terms $f_1 = f_2 = 0$. Only Dirichlet boundary conditions are used in this problem. The system is augmented with the following boundary conditions:

$$\begin{aligned} &\phi = 5.0\,\mathrm{V} \quad \text{on } \Gamma^1_{D,\phi}, \quad \text{and} \quad \phi = 0.0\,\mathrm{V} \quad \text{on } \Gamma^2_{D,\phi}, \\ &c_i = 1.0\,\mathrm{M} \quad \text{on } \Gamma^1_{D,c}, \quad \text{and} \quad c_i = 0.0\,\mathrm{M} \quad \text{on } \Gamma^2_{D,c}, \ i = 1, 2, \end{aligned}$$

where $\Gamma^1_{D,\phi} = \{(x, y, z)\,|\,x = 50 \text{ or } y = 50 \text{ or } z = 50\}$, $\Gamma^2_{D,\phi} = \partial\Omega \backslash \Gamma^1_{D,\phi}$, $\Gamma^1_{D,c} = \{(x, y, z) \mid z = 50\}$, and $\Gamma^2_{D,c} = \partial\Omega \backslash \Gamma^1_{D,c}$.

We have computed the numerical solution with three methods: the standard FE, SUPG and SUPG–IP methods. The concentration distributions of K^+ and Cl^- on the yOz cut plane are displayed in Figs. 2 and 3, respectively. The numerical solution of the standard FE method suffers from spurious oscillations, making the results unusable (see the left columns). The SUPG method significantly depresses oscillations but still has some unreasonable overshoots and undershoots, resulting in the presence of negative concentrations. In contrast, the SUPG–IP method effectively obviates nonphysical oscillations and has the least overshoots and undershoots, with all the ionic concentrations staying positive.

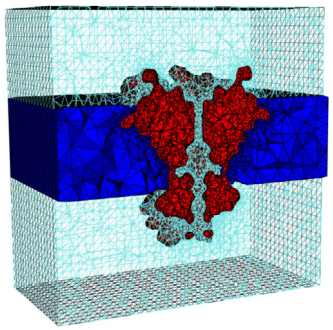

Fig. 4. The unstructured tetrahedral volume mesh for the KcsA ion channel. The membrane region is colored blue and the protein region is colored red. The rest is the solvent region.

3.2. Simulations of the KcsA ion channel

The mechanism study of ion transport through channel proteins is a vital application of the PNP model. Several different ion channels include GA [Protein Data Bank (PDB) ID: 1MAG], VDAC [PDB ID: 2JK4] and PA [PDB ID: 1V36] have been simulated with FE methods and their macroscopic properties like current–voltage characteristics and ion conductance were analyzed in the previous works [14–16]. Our focus in this work is on the stability and robustness of the FE methods. Thus, the challenging KcsA K^+ channel [PDB ID: 1BL8] is selected for our simulations.

The channel protein consists of 5892 atoms, with three primary sections: an opening pore on the cytoplasmic side of the cell interior, a large water-filled cavity, and a narrow selectivity filter [16]. The unstructured tetrahedral volume mesh for the KcsA ion channel used in our experiment is shown in Fig. 4. The mesh over the whole domain has a total of 73174 vertices and 441475 tetrahedral elements. The complicated surface geometry and highly charged protein often lead to difficulties in convergence of numerical solution.

To investigate the robustness of these methods, we design two groups of experiments. In the first group, we fix the potential difference between the top and bottom faces of the simulation box to 0.1 V. Then, we increase the bulk concentrations and watch the convergence performance of the three methods: the standard FE, SUPG and SUPG–IP methods. In the second group, similarly, we fix the bulk concentrations to 0.1 M and vary the potential difference between the top and bottom faces of the simulation box.

Table 2 displays the convergence performance and numbers of Gummel iterations of the three methods under different bulk concentrations and voltages. The maximum number of Gummel iterations is set to 1000. “Fail” means failing to converge. To further test the stability and robustness of these FE methods, we increase the bulk concentrations in the first group up to 4.5 M and the voltages in the second group up to 25 V. Although these conditions seem unreasonable in ion channel systems, they can be common in other systems which share analogous models, for instance, large biases in simulations of semiconductor devices [17] and high concentration electrolyte solutions in simulations of nanopores, and the KcsA ion channel is taken as a representative to illustrate the convergence problem of the FE methods for the PNP model. As can be seen, the standard FE method fails to converge in most cases. The SUPG method can deal with a much wider range of bulk concentrations and voltages than the standard FE method. Nevertheless, the SUPG–IP method demonstrates the best performance in convergence, especially when the voltages applied are very high, which manifests the great advantages of this novel scheme. Table 2 shows that the numbers of Gummel iterations of these methods are similar under most conditions. We here list the CPU time cost under two conditions: $voltage = 0.1$ V, $c_{i,bulk} = 0.05$ M and $voltage = 2$ V, $c_{i,bulk} = 0.1$ M. The CPU time cost by the standard FE method with 128 MPI processes is 148.10 s and 134.90 s respectively, while the corresponding

Table 2
Number of Gummel iterations of the three FE methods.

$voltage$ = 0.1 V				$c_{i,bulk}$ = 0.1 M			
$c_{i,bulk}$ (M)	Standard FE	SUPG	SUPG–IP	$voltage$ (V)	Standard FE	SUPG	SUPG–IP
0.05	202	204	203	0.5	310	286	244
0.1	198	200	197	1	253	222	232
0.15	Fail	200	199	2	198	199	198
0.5	Fail	197	199	4.2	1000	199	199
2	Fail	197	198	15	Fail	200	198
2.8	Fail	197	193	18	Fail	215	198
3	Fail	Fail	210	19	Fail	Fail	198
4.5	Fail	Fail	206	25	Fail	Fail	198

time cost by the SUPG–IP method is 165.84 s and 149.47 s. Overall, the SUPG–IP method only adds a little bit more computation relative to the standard FE method.

4. Conclusions

In this work, we propose a novel stabilized finite element method to solve the PNP equations. The example problem with an analytical solution verifies the accuracy and convergence rate of our method. Further numerical experiments demonstrate the advantages of the novel method in preventing numerical oscillations and preserving positivity. Simulations of the KcsA channel protein system confirm its applicability in a realistic setting, and results show that the SUPG–IP method performs much better in terms of stability and robustness than the standard FE and SUPG methods. The SUPG–IP method succeeds in converging under conditions of much higher bulk concentrations and membrane potentials than previous FE methods, even for highly charged protein molecules like KcsA. Moreover, the method and program can be utilized in other systems sharing analogous models such as semiconductor devices and nanopores as well. Our future work includes exploring applicability of this method to other modified PNP models or alternative formulations, and further numerical analysis of the method for PNP solution.

CRediT authorship contribution statement

Qin Wang: Methodology, Software, Writing - original draft, Writing - review & editing. **Hongliang Li:** Conceptualization, Writing - review & editing. **Linbo Zhang:** Software, Writing -review & editing. **Benzhuo Lu:** Conceptualization, Writing - review & editing.

Acknowledgments

The authors thank Sheng Gui and Jingjie Xu for their help in mesh generation and coding. This work is supported by Science Challenge Project (Grant No. TZ2016003), National Key Research and Development Program of China (Grant No. 2016YFB0201304), and National Natural Science Foundation of China (Grant No. 21573274, 11771435).

References

[1] Q.F. Zhong, Q. Jiang, P.B. Moore, D.M. Newns, M.L. Klein, Molecular dynamics simulation of a synthetic ion channel, Biophys. J. 74 (1) (1998) 3–10.
[2] M.E. Davis, J.D. Madura, B.A. Luty, J.A. McCammon, Electrostatics and diffusion of molecules in solution - simulations with the University-of-Houston-Brownian Dynamics program, Comput. Phys. Comm. 62 (2–3) (1991) 187–197.
[3] W.V. Roosbroeck, Theory of the flow of electrons and holes in germanium and other semiconductors, Bell Syst. Tech. J. 29 (4) (1950) 560–607.

[4] R.J. French, Finite Difference Methods for the Numerical Solution of the Nernst-Planck-Poisson Equations, Springer Berlin Heidelberg, 1974, pp. 50–61.
[5] J. Fuhrmann, C. Guhlke, A finite volume scheme for Nernst-Planck-Poisson systems with ion size and solvation effects, in: Springer Proceedings in Mathematics & Statistics, vol. 200, Springer, 2017, pp. 497–505.
[6] B. Lu, M.J. Holst, J.A. McCammon, Y.C. Zhou, Poisson-Nernst-Planck equations for simulating biomolecular diffusion-reaction processes I: Finite element solutions, J. Comput. Phys. 229 (19) (2010) 6979–6994.
[7] T. Liu, S. Bai, B. Tu, M. Chen, B. Lu, Membrane-channel protein system mesh construction for finite element simulations, Mol. Based Math. Biol. 3 (1) (2015) 128–139.
[8] T. Liu, M. Chen, B. Lu, Efficient and qualified mesh generation for Gaussian molecular surface using adaptive partition and piecewise polynomial approximation, SIAM J. Sci. Comput. 40 (2) (2018) B507–B527.
[9] A.N. Brooks, T.J.R. Hughes, Streamline upwind/Petrov–Galerkin formulations for convection dominated flows with particular emphasis on the incompressible Navier–Stokes equations, Comput. Methods Appl. Mech. Engrg. 32 (1–3) (1982) 199–259.
[10] J. Douglas, T. Dupont, Interior Penalty Procedures for Elliptic and Parabolic Galerkin Methods, Springer Berlin Heidelberg, 1976, pp. 207–216.
[11] E. Burman, P. Hansbo, Edge stabilization for Galerkin approximations of convection–diffusion-reaction problems, Comput. Methods Appl. Mech. Engrg. 193 (15–16) (2004) 1437–1453.
[12] H. Duan, Y. Wei, A New Edge Stabilization Method for the Convection-Dominated Diffusion-Convection Equations, Springer International Publishing, 2018, pp. 48–60.
[13] L. Zhang, A parallel algorithm for adaptive local refinement of tetrahedral meshes using bisection, Numer. Math. Theory Methods Appl. 2 (1) (2009) 65–89.
[14] B. Tu, M. Chen, Y. Xie, L. Zhang, R.S. Eisenberg, B. Lu, A parallel finite element simulator for ion transport through three-dimensional ion channel systems, J. Comput. Chem. 34 (24) (2013) 2065–2078.
[15] B. Tu, Y. Xie, L. Zhang, B. Lu, Stabilized finite element methods to simulate the conductances of ion channels, Comput. Phys. Comm. 188 (2015) 131–139.
[16] X. Liu, B. Lu, Incorporating born solvation energy into the three-dimensional Poisson-Nernst-Planck model to study ion selectivity in KcsA K^+ channels, Phys. Rev. E 96 (2017) 062416.
[17] J. Miller, W. Schilders, S. Wang, Application of finite element methods to the simulation of semiconductor devices, Rep. Progr. Phys. 62 (3) (1999) 277–353.